

Design of a VTOL UAV for anti-poaching surveillance missions in the Danube Delta

First A. Sorin Andrei NEGRU, Second B. Marilena MANEA, and Third C. Gabriel JIGA

Abstract— In order to decrease the poaching activity in the Danube Delta it is possible to implement an unmanned aerial vehicle (UAV) using a vertical take-off and landing (VTOL) configuration destinated to an easily deployment for a short-range surveillance mission with a fully electrical power system. A lightweight structure therefore is needed with a good stiffness-weight ratio for a better flight autonomy. After the design process the presented drone reached an acceptable overall mass and the constrains imposed by the authors resulted suitable.

Index Terms— Danube Delta, Environment, poaching, surveillance.

I. INTRODUCTION

The unmanned aerial vehicles have gained a relevant importance along different research departments from all around the world, due to the technological progress. Indeed, the drones can solve a vastly number of problems and considering that the flora and the fauna are the most important things for the humanity due to its impact over the world, it is, consequently our duty to secure and protect our local biodiversity. Romania, in these terms with the Danube Delta has a rich ecosystem diversity, where are living different species among which the sturgeon, that is the most vulnerable and exposed fish to extinction. Considering that worldwide there are 27 different species of sturgeon and only 6 could be found in the Danube [1], it is important to discourage any poaching attempts. To achieve this, it is important to set a proper set of rules and to assure that these rules are respected. The mostly widespread applications of the drones are correlated with the surveillance of the sensible areas and in this purpose the implementation of a VTOL drone may be considered. This kind of drone configuration is particularly interesting for its flying features. It is a combination between a fixed wing drone, obtaining in consequence a long endurance, due to the wing, that generates the mayor quantity of lift force and a copter drone, that can lead to a faster deployment, in any environment, due to its ability to take-off vertically. The main advantage of using a drone to solve the poaching problem is the speed at which the drone is flying, because it can easily detect any suspect fisher in a small amount of time, and further the fisher can be intercepted by the local authorities. As disadvantage, may be even the local fauna, because considering that the Danube is the home of hundreds of bird's species, this may be a problem when

flying, risking a bird strike. In case, of any possible impact that can lead the drone to a possible crash, it is recommended to choose a safer configuration when flying, introducing a coaxial quadrotor [2] drone configuration, to switch, in case of impact, from the fixed wing configuration.

II. STANDARD SURVEILANCE FLIGHT PLAN

A typical surveillance flight plan using a Mission Planner interface can be viewed in fig.1. The achieved autonomy, in the software in the loop (SITL) simulation performed in the Danube Delta is equivalent to nearly 15 km, being the target autonomy of the drone, that it is acceptable, considering the fully electrical power system used and the overall budged.



Figure 1 Surveillance flight plan in Mission Planner for a VTOL drone

The drone, in the first stage is hovering from a boat in copter mode, until reaching the target altitude of 40 m. At this point the motors of the drone in copter mode, will stop, executing a transition from the copter mode to the fixed wing configuration, reaching more easily each waypoint. Finally, at the last waypoint the drone is performing the transition from the fixed wing mode to the copter mode, landing safely to the boat.

Table I Flight phases

Number	Flight Phase
1	Take-off Vertically
2	VTOL transition to fixed wing mode
3	Waypoint navigation
4	VTOL transition to copter mode
5	Landing Vertically

III. FIRST WEIGHT ESTIMATION FOR A VTOL DRONE

To achieve the proposed autonomy, the drone needs to be light and strength, with an imposed initial mass, by the

This work was supported by S.A.N Author.

S. A. N Author was with Equipment and Aviation Systems Department, Politehnica University of Bucharest, 011061 RO. He is now with the Nuclear NDT Research and Services, Bucharest 041919 RO (e-mail: negrusorin28@yahoo.it).

M. M. was with Aerospace Construction, "Elie Carafoli" Department, Politehnica University of Bucharest, 011061 RO. She is now with the

Institute for Theoretical and Experimental Analysis of Aeronautical-Astronautics Structures, Bucharest 061126 RO (e-mail: marilena.manea31@gmail.com).

G. J. Professor at Strength of Materials Department, Faculty of Industrial Engineering and Robotics, Politehnica University of Bucharest, 011061 RO. (gabriel.jiga@upb.ro)

authors, of 2.5 kg that can be split in three parts. The first one is composed by the electrical components for the vertical flight (W_e), the second one by the electrical components for the fixed wing mode (W_{efw}) and the last one by the overall structure weight (W_{str}).

$$W_t = W_{str} + W_{efw} + W_e \quad (1)$$

Using the online eCalc [3] website, it is possible, to select all the necessary components required to perform the vertical flight verifying in this way how suitable are the selected components for the given drone mass.

Table II Electrical components for the vertical flight selected from eCalc

Quantity	Component	Mass [g]
1	Pixhawk 2.4	38
1	500mW Holybro Telemetry 433 MHz	11.5
8	EMAX MT2213 935 KV	424
8	ESC 30A	200
1	Li-Po 3S 6000 mAh 30C	356
5	SG 90 Servo motor	45
1	Pitot Tube	18.1
1	Eachine1000TVL camera	10.4
1	TS832 AV Transmitter	22
1	Power module XT60	17
1	Pixhawk cables	22
1	GPS and compass	34
8	Aeronaut CamCarbon 12x6 propeller	56
Total		1254

A much lighter drone configuration may be obtained but considering any future failure of any electronic speed controller (ESC), it is preferable to use 8 motors instead of 4. The unknown mass of the electrical components for the fixed wing configuration can be obtained once the total area of the wing is obtained, and to achieve that, it is necessary firstly to select an adequate wing airfoil to obtain all the necessary coefficients needed for the design space graph.

IV. AIRFOIL SELECTION

To choose an appropriate wing airfoil, the authors selected 5 airfoils from UIUC database [4] from where it is possible to extract the coordinates of the points that form the selected airfoils. Another condition, in this selection phase, is to find an airfoil with a flat lower surface necessary for the installation of 2 carbon fiber tubes used to mount all the electrical motors and the horizontal and vertical tails. The airfoils selected are: Rhode 32 (number 1), Rhode 34 (number 2), Clark Y (number 3), Drela AG36 (number 4) and Drela AG38 (number 5). For a range of Reynolds number between $2 \cdot 10^4$ and $4 \cdot 10^6$ and an angle of attack (AOA) between -10° and 30° , using the XFLR5 software, a number of dependencies between lift and drag coefficient, also between lift coefficient and angle of attack were obtained for each airfoil. These dependencies are illustrated in fig.2 and fig.3.

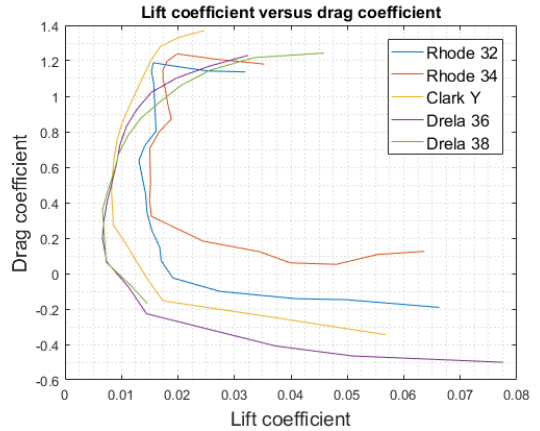


Figure 2 The variation of the lift coefficient versus the drag coefficient for the selected airfoils

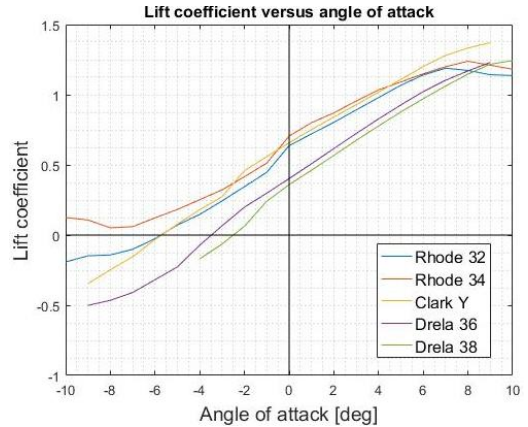


Figure 3 Variation of the lift coefficient with the angle of attack (AOA)

The results of the analysis showed that Clark-Y adequately met the requirements, so it was chosen as the main wing airfoil.

Table III Airfoils characteristics

Re for cruise	$2.9 \cdot 10^5$				
Airfoil	1	2	3	4	5
Thickness	0.119	0.14	0.116	0.08	0.07
C_L for AOA=0	0.635	0.706	0.658	0.403	0.36
$C_{L_{max}}$	1.189	1.239	1.379	1.231	1.244
AOA for $C_{L_{max}}$	7	8	10	9	10
$C_{D_{min}}$	0.013	0.015	0.004	0.007	0.007
C_L for $C_{D_{min}}$	0.637	0.322	0.459	0.067	0.064
$\left(\frac{C_L}{C_D}\right)_{max}$	73.73	66.24	83.76	73.32	70.98
C_L for $\left(\frac{C_L}{C_D}\right)_{max}$	1.188	1.15	0.841	0.828	0.675

V. CONSTRAIN PARAMETERS

After the selection process of the different airfoils, the next step was to perform a constrain analysis. In this way it is possible to set the optimal wing surface area and the thrust/weight ratio (T/W) [5] - [6], indispensable parameter, for a stable flight. So, to obtain and to extract all the necessary data it is necessary to plot a design space graph with some input parameters. To obtain a stable image in flight, a cruise speed (V_c) of 20 m/s is selected and, in this way, it is possible to obtain [6] the climb speed (V_u) and the stall speed (V_s).

$$V_u = V_c \cdot 0.8 \quad (2)$$

$$V_s = \frac{\left(\frac{V_c}{2}\right)}{1.1} \quad (3)$$

Table IV Input data

Nr.	Input parameters	Value
1	Cruise speed (V_c)	20 (m/s)
2	Estimated Climb speed (V_u)	16 (m/s)
3	Estimated Stall speed (V_s)	9.09 (m/s)
4	Minimum drag coefficient (CD_{min})	00.4
5	Maximum lift coefficient (CL_{max})	1.3
6	Aspect Ratio (AR)	7
7	Rate of climb (V_v)	5 (m/s)
8	Bank angle (ϕ)	45 (deg)

The two-dimensional graph is composed by different flying conditions, obtaining after the final combination, an acceptable area, from where it is possible to extract a good thrust/weight ratio and a weight/surface ratio (W/S). The first condition defines the thrust/weight ratio when the drone is engaged in a level turn at a specific load factor, with a constant cruise speed and altitude, as defined in (4).

$$\frac{T}{W} = q_c \cdot \left[C_{Dmin} \cdot \left(\frac{W}{S_w} \right) + k \cdot \left(\frac{n}{q_c} \right)^2 \cdot \left(\frac{W}{S_w} \right) \right] \cdot 0.101971621 \quad (4)$$

Where:

- q_c = dynamic pressure during cruise speed (Pa)
- k = lift-induced drag constant
- S_w = wing area (m^2)
- n = load factor

The second condition defines the required T/W ratio necessary, to achieve the rate of climb defined before, using formula (5).

$$\frac{T}{W} = \frac{Vv}{V_u} + \frac{q_u}{W/S_w} \cdot C_{Dmin} + \frac{k}{q_u} \cdot \left(\frac{W}{S_w} \right) \cdot 0.101971621 \quad (5)$$

Where:

- q_u = dynamic pressure during climb speed (Pa)

The third condition, using the cruise speed defined in table V, is used, in this case, to obtain the necessary thrust-weight ratio as specified in (6).

$$\frac{T}{W} = q_c \cdot C_{Dmin} \cdot \left(\frac{1}{W/S_w} \right) + k \cdot \left(\frac{1}{q_c} \right) \cdot \left(\frac{W}{S_w} \right) \cdot 0.101971621 \quad (6)$$

In addition, a wing loading (W/S) constrain is defined by formula (7)

$$\frac{T}{W} = \frac{1}{2} \cdot \rho_{40} \cdot V_s^2 \cdot C_{Lmax} \quad (7)$$

Where:

- ρ_{40} = density of the air at an altitude of 40 m

Finally, from the combination of all the conditions imposed, in fig. 4, in the acceptable region, selecting an equivalent

value of the thrust-weight ratio of 0.151 it can be obtained the total wing loading (W/S), that in this case is 6.6 kg/m².

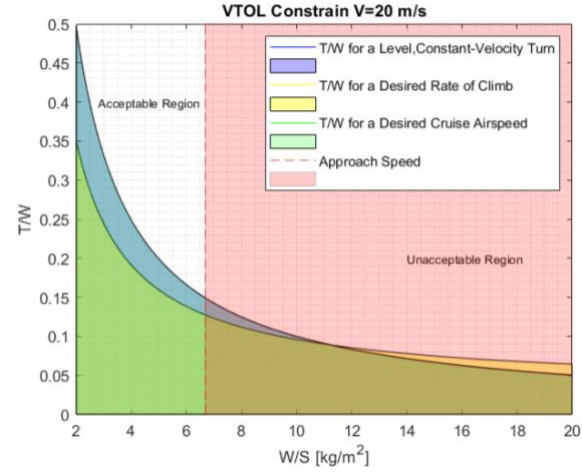


Figure 4 Design Space graph

Using the formula (8) with the wing loading from fig.3 it is possible, with an estimated initial weight, to obtain the total wing surface area (S_w).

$$S_w = \frac{W}{W/S_w} \quad (8)$$

Consequently, if $W = 2.5$ (kg) an equivalent wing surface area (S_w) of 0.37 m² will be obtained.

VI. VTOL STRUCTURE DESIGN

Considering a rectangle wing, with an imposed aspect ratio (AR) of 7 it is possible to obtain the wing span (b_w), the chord of the wing (c_w) the length (L_{ail}) [7] and the width (l_{ail}) [7] of the ailerons.

$$b_w = \sqrt{S_w \cdot AR} \quad (9)$$

$$c_w = \frac{b_w}{AR} \quad (10)$$

$$L_{ail} = b_w \cdot \frac{40}{100} \quad (11)$$

$$l_{ail} = c_w \cdot \frac{25}{100} \quad (12)$$

Once obtained all the main design data for the wing, two carbon fiber tubes are used as spars, to ensure the wing strength, with an equivalent diameter of 10 mm and respectively 7 mm with a distance between them of 75 mm.

Table V Rectangle Wing design features

Parameter	Value
S_w	0.37 (m^2)
AR	7
b_w	1.6 (m)
c_w	0.22 (m)
L_{ail}	0.66(m)
l_{ail}	0.055 (m)
Ribs distance	0.05 (m)
First Spar diameter	0.01 (m)
Second Spar diameter	0.0075 (m)
Distance between spars	0.075 (m)
Ribs thickness	0.003 (m)

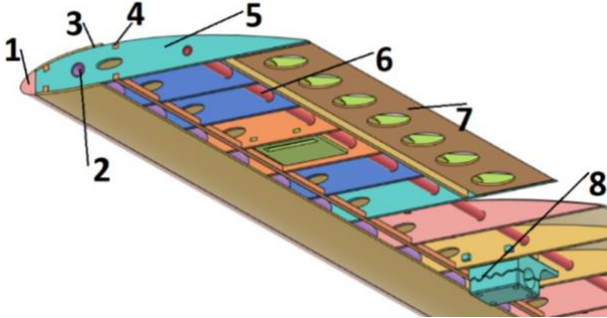


Figure 5 Main wing section; 1- Balsa Leading Edge; 2- First CFRP spar; 4 – Stringer; 5 Rib; 6 – Second CFRP spar; 7 – Aileron; 8 – 3D printed component

Furthermore, 4 balsa strings were used to confer more strength to the wing and a balsa leading edge was used to simplify the mount of the balsa skin layer of 1.5 mm [8]. Additionally, two 3D printed components made by Polylactic Acid (PLA) are used to connect the carbon fiber tubes of 10 mm diameter, as connectors, where to mount all the brushless motors for the vertical flight and the horizontal and vertical tails.

The fuselage is the main structure where are located all the navigation sensors and it is important to design it, to allow enough space for all the necessary components. In these terms it is important to know previously the dimensions of the interested electrical components and to design around them the desired fuselage shape, obtaining from the CAD software an equivalent fuselage length, of 0.540 m and a total weight of 426 g.

For this application the authors selected a NACA 0010 airfoil to be implemented in the design of the tails. The aspect ratio of the horizontal tail (AR_{HT}) [9] was obtained using [13], in addition a horizontal tail volume coefficient (V_{HT}) of 0.6 [10] is considered.

Where:

- S_{HT} = Horizontal tail surface (m^2) [11];
- b_{HT} = Horizontal tail span (m) [11];
- c_{HT} = Horizontal tail chord (m);
- l_{HT} = Elevator chord (m);
- L_{HT} = Horizontal tail arm moment (m) from the center of gravity of the main wing to the center of gravity of the horizontal tail [11];

$$AR_{HT} = AR \cdot \frac{2}{3} \quad (13)$$

$$S_{HT} = \frac{V_{HT} \cdot S_w \cdot c_w}{l_{HT}} \quad (14)$$

$$b_{HT} = \sqrt{S_{HT} \cdot AR_{HT}} \quad (15)$$

$$c_{HT} = \frac{b_{HT}}{AR_{HT}} \quad (16)$$

$$l_{HT} = c_{HT} \cdot \frac{25}{100} \quad (17)$$

$$L_{HT} = \frac{V_{HT} \cdot S_w \cdot c_w}{S_{HT}} \quad (18)$$

To increase the strength of the horizontal tail, two carbon fiber tubes of 4 mm are used, and finally the entire structure is covered with a transparent film, in order to decrease its

weight, reducing the amount of balsa used commonly to cover it.

Table VI Horizontal tail design features

Parameter	Value
AR_{HT}	4.6
S_{HT}	0.083 (m^2)
b_{HT}	0.62 (m)
c_{HT}	0.13 (m)
l_{HT}	0.039 (m)
L_{HT}	0.588 (m)
Spar diameter	0.004 (m)
Distance between spars	0.048 (m)

The next step is to define the two vertical tails dimensions with an equivalent tail volume (V_{VT}) of 0.0368 from [10] and an aspect ratio (AR_{VT}) of 1.8 from [12].

$$S_{VT} = 0.1 \cdot S_w \quad (19)$$

$$b_{VT} = \sqrt{S_{VT} \cdot AR_{VT}} \quad (20)$$

$$c_{rVT} = \frac{b_{VT}}{AR_{VT}} \quad (21)$$

$$c_{tVT} = \frac{c_{rVT}}{TR_{VT}} \quad (22)$$

$$MAC_{VT} = \frac{2}{3} \cdot c_{rVT} \cdot \frac{TR_{VT}^2 + TR_{VT} + 1}{(TR_{VT} + 1)} \quad (23)$$

$$L_{VT} = \frac{V_{VT} \cdot S_w \cdot b_w}{S_{VT}} \quad (24)$$

$$l_r = c_{rVT} \cdot \frac{25}{100} \quad (25)$$

Where:

- S_{VT} = Vertical tail surface area (m^2) [13];
- b_{VT} = Vertical tail span (m);
- c_{rVT} = Root tail chord length (m);
- c_{tVT} = Tip tail chord length (m);
- TR_{VT} = Taper ratio;
- MAC_{VT} = Mean aerodynamic chord of the vertical tail (m);
- L_{VT} = Vertical tail arm moment from the center of gravity of the main wing to the center of gravity of the vertical tail (m);
- l_r = Rudder width (m);

Table VII Vertical tail design

Parameter	Value
S_{VT}	0.037 (m^2)
b_{VT}	0.25 (m)
c_{rVT}	0.14 (m)
c_{tVT}	0.1 (m)
TR_{VT} (estimated)	1.35
MAC_{VT}	0.2 (m)
L_{VT}	0.588 (m)
l_r	0.035 (m)

VII. FINAL WEIGHT ESTIMATION

With the equivalent wing surface obtained from fig.4, it is possible to estimate the total mass of the electrical

components required for the fixed wing configuration, using the eCalc software.

Table VIII Electrical components for required the horizontal flight from eCalc

Components	Mass [g]
Picher Boost 30 1130 KV	163
ESC 40 A	9.6
Aeronaut CamCarbon 9x6 propeller	7
Total	179.6

Once designed all the structural components of the drone it is possible to extract their weight from the CAD software, for a first preview of the structure weight, obtaining consequently an overall drone mass of 2614.6 g that is acceptable.

Table IX Structure Weight

Quantity	Components	Mass [g]
2	Vertical tails	50
1	Horizontal tail	72
1	Wing	450
1	Fuselage	426
2	Landing gear	183
Total		1181

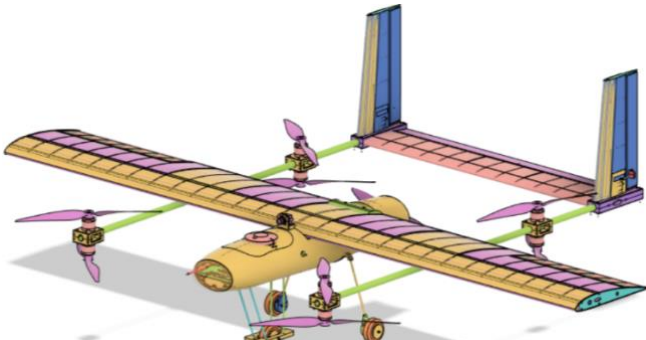


Figure 6 Overall VTOL design

VIII. CONCLUSION AND FURTHER WORK

The obtained final drone mass, from a first preview is acceptable, and the practical development of the drone will confirm it. The next step to finish the design, is to obtain the centre of gravity of the drone with an experimental stand where to put the drone and in this way will be possible to allocate correctly the position of the landing gear.

CONFLICT OF INTEREST

"The authors declare no conflict of interest".

AUTHOR CONTRIBUTIONS

S.A.N conducted the research regarding the flight plan and the electrical components, instead M.M managed all the structural design.

IX. REFERENCES

- [1] „LIFE FOR DANUBE STURGEONS” . Available: <https://danube-sturgeons.org/how-to-help/>.
- [2] K. G. B. a. Y. K. Gilar Budi Raharja, „Design and implementation of coaxial quadrotor for an autonomous outdoor flight”, in *International Conference on Ubiquitous Robots and Ambient Intelligence (URAI)*, Incheon, Korea (South), 2011.
- [3] M. Müller, „eCalc,” 2020 05 13. Available: <https://www.ecalc.ch/xcoptercalc.php>.
- [4] „UIUC Applied Aerodynamics Group, Department of Aerospace Engineering,” 2020. Available: https://m-selig.ae.illinois.edu/ads/coord_database.html.
- [5] S. Gudmundsson, „General Aviation Aircraft Design: Applied Methods and procedures,” Embry-Riddle Aeronautical University, Elsevier, 2014, pp. ch. 3, pp. 57-59.
- [6] A. J. K. A. S. J. P. Scanlan, „Small Unmanned Fixed-wing Aircraft Design: A Practical Approach,” University of Southampton, UK, John Wiley & Sons Ltd, 2017, pp. cap.10, pp.154-159.
- [7] A. Lennon, „Basics of R/C Model Aircraft Design: Practical Techniques for Building Better Models,” Ridgefield, Air Age Media, 1996, p. pg. 49.
- [8] A. Lennon, „Basics of R/C Model Aircraft Design: Practical Techniques for Building Better Models,” Ridgefield, Air Age Media, 1996, p. pg. 66.
- [9] M. Sadraey, „Tail Design,” Daniel Webster College, p. 323.
- [10] „Lab 8 Notes – Basic Aircraft Design Rules”.
- [11] S. Gudmundsson, „General Aviation Aircraft Design Applied Methods and Procedures,” Elsevier, 2014, p. 503.
- [12] D. Stinton, „Design of the Aeroplane, 2nd Edition,” London: Collins (1985) Reprint, 1985, p. pg. 417.
- [13] M. H. Sadraey, „Aircraft Design: A Systems Engineering Approach,” WILEY, 2012, p. pg. 324.

Copyright © 2021 by the authors. This is an open access article distributed under the Creative Commons Attribution License which permits unrestricted use, distribution, and reproduction in any medium, provided the original work is properly cited ([CC BY 4.0](https://creativecommons.org/licenses/by/4.0/)).



Sorin Andrei Negru (Tecuci, 1998) studied at Instituto Tecnico Aeronautico "Antonio Locatelli", Bergamo in Italy. He moved to Romania, at University Politehnica of Bucharest, where he achieved a bachelor's degree in aerospace engineering, equipment and aviation systems. During his bachelor, he had an internship at TU Berlin, DAI-Lab, Germany, where he worked and developed autonomous drones combined with artificial intelligence (AI). In addition, during the university period, was the team leader of group of students, with the purpose, to study a possible electrification of a BN-2 aircraft in collaboration with Romaero and University Politehnica of Bucharest (UPB). He is a research electrical engineer at Nuclear NDT Research & Services.



Marilena Manea (Galati, 1997) received the bachelor's degree in aerospace engineering from the Polytechnic University from Bucharest, Romania in 2020. She is a M.Sc. degree candidate in the “Elie Carafoli” Aerospace Science department at UPB. She is currently working as Aerospace Construction Research Engineer at the Institute for Theoretical and Experimental Analysis of Aeronautical-Astronautics Structure involved in SICABA project.



Gabriel Jiga (Bucharest, 1961) obtained his PhD Degree in Industrial Engineering (1997) and Bachelor of Science Degree in Machine Building Technology (1986) - Faculty of Engineering and Management of Technological Systems, POLITEHNICA University of Bucharest, (Romania). At present he is full professor at the Strength of Materials Department and PhD supervisor. His field of interest is linked to the experimental stress analysis, numerical methods, finite element modelling applied on layered composite structures, sandwich materials, low velocity impact modelling.